ISSN: 1392-6292/ eISSN: 1648-3510

VILNIUS TECH
Vilnius Gediminas Technical University

MATHEMATICAL MODELLING and ANALYSIS

2026
Volume 31
Issue 2
Pages 267–287
https://doi.org/10.3846/mma.2026.24857

A successive midpoint-based method for the numerical analysis of chaotic systems with local and nonlocal operators

Seda İğret Araz[a] and Mehmet Akif Çetin[b] ✉

[a] *Department of Mathematics Education, Siirt University, 56100 Siirt, Turkey*

[b] *ALTSO Vocational School, Alanya Alaaddin Keykubat University, 07450 Alanya, Turkey*

Article History:

- received September 17, 2025
- revised December 1, 2025
- accepted January 28, 2026

Abstract. In this study, we examine the uniqueness conditions for solutions of fractal differential equations using the Krasnoselskii-Krein uniqueness theorem. The analysis establishes sufficient criteria that guarantee the existence of unique solutions. Additionally, we employ the successive midpoint method to numerically solve chaotic systems governed by both fractal and global derivatives. To evaluate the effectiveness of the proposed approach, graphical simulations are presented for various derivative orders. These results illustrate the method's accuracy, stability, and reliability in capturing the intricate dynamics of the considered systems.

Keywords: fractal differential equations; Krasnoselskii-Krein uniqueness theorem; successive midpoint method.

AMS Subject Classification: 28A80; 34A12; 65L05.

✉ Corresponding author. E-mail: akif.cetin@alanya.edu.tr

1 Introduction

A wide range of real-world phenomena are modeled by mathematical formulations that are too complex to solve analytically. The lack of closed-form solutions for differential equations, integrals, and systems of equations necessitates the use of numerical methods for practical analysis and simulation [1,2,3,4,5,6]. Fields such as weather prediction, financial market modeling, and the simulation of physical systems rely extensively on numerical approximations to generate reliable results. Numerical methods make it possible to compute solutions for large-scale, complex problems within a reasonable time frame, often with high precision and accuracy. Techniques such as iterative solvers, finite element methods, and interpolation algorithms enable numerical results to closely match empirical observations. This level of precision is especially critical in engineering applications, where even small errors can have significant

consequences. The adaptability of numerical methods allows their use across numerous disciplines, including the solution of partial differential equations in physics, optimization in computer science, and statistical modeling in biological research. With the advent of high-performance computing and parallel processing, the simulation and analysis of previously intractable systems have become feasible, continuously expanding the scope and impact of numerical computation. Furthermore, learning and applying numerical methods equips students and researchers with essential analytical and problem-solving skills, fostering a deeper understanding of the underlying mathematical principles [7, 8, 9, 10].

Local operators, which act on values in the immediate neighborhood of a point, are fundamental in various areas of science and engineering. These operators are central to differential and integral calculus, linked by the fundamental theorem of calculus, and are crucial for analyzing functions, signals, and data. More generalized forms of local operators have been introduced in recent years, including the fractal derivative, which allows differentiation of non-integer order and captures local irregularities in functions with fractal characteristics [8]. Another notable extension is the Caputo–Fabrizio (CF) derivative [7], which involves a convolution of the rate of change with an exponential-type kernel, enabling memory effects without singular kernels. Fractal derivatives [8], like their classical counterparts, provide information about the behavior and variation of a function near a given point, but they do so in a way that more effectively captures local complexity. These derivatives can take various forms, each tailored to represent specific local properties of irregular or complex functions.

In recent years, the classical notion of instantaneous change has been generalized to address the limitations of traditional derivatives in modeling complex real-world phenomena. This generalization led to the development of a broader differential operator, commonly referred to as the global derivative, which is constructed to be compatible with the Riemann–Stieltjes integral. A key feature of this framework is that, by selecting appropriate generating functions, one can recover all existing local differential operators defined through conventional rates of change. Although the global derivative remains a relatively new concept, ongoing research aims to establish a comprehensive Riemann–Stieltjes–based calculus to support its theoretical foundations. The global derivative extends differentiation by allowing the rate of change of a function to be measured with respect to another positive, strictly increasing, and non-constant function. This structure enables the operator to capture more intricate dynamics, making it suitable for complex systems where classical derivatives fail to provide accurate descriptions. This framework has been shown to be equivalent to the Riemann–Stieltjes integral, which generalizes the classical Riemann integral by allowing integration with respect to a non-constant function [2].

Since such generalized derivatives provide advanced tools for modeling and analyzing chaotic dynamics, it is imperative to develop and apply robust and accurate numerical methods to solve equations involving them [1, 10]. In this study, we focus on the application of the successive midpoint method, as proposed by Atangana and Araz in [4], to chaotic systems governed by fractal,

Caputo–Fabrizio, and global fractional derivatives. In their work, Atangana and Araz developed a numerical scheme based on subdividing the domain into successive intervals and applying the midpoint approach to solve nonlinear ordinary differential equations involving both classical and Caputo–Fabrizio operators. Their findings demonstrated that the midpoint-based scheme significantly improves solution accuracy. Furthermore, in a related study [3], the authors extended their analysis to a class of stochastic differential equations involving newly defined global derivatives of both integer and non-integer orders. They provided numerical schemes tailored to each operator class and conducted thorough error analyses to validate the performance of their methods. The primary objective of this study is to investigate the effectiveness of the successive midpoint method in solving a class of chaotic systems governed by differential equations involving classical, Caputo–Fabrizio (CF), fractal, and global derivatives [5]. By implementing the method across different types of fractional operators, we aim to evaluate its numerical accuracy and applicability to complex dynamical systems. Special attention is also given to the case of fractal derivatives, for which the theoretical conditions ensuring the uniqueness of solutions are analyzed using the Krasnoselskii–Krein fixed-point framework.

In this paper, the successive midpoint method—originally formulated for classical and Caputo–Fabrizio derivatives—is systematically extended to encompass differential equations involving fractal and global derivative operators, thereby broadening its applicability to a wider class of nonlocal and generalized dynamical models. The method's performance is rigorously evaluated on chaotic systems governed by these operators, enabling a comprehensive assessment of its numerical accuracy and its capability to faithfully capture intricate dynamical behaviors. Moreover, for the case of fractal differential equations, the uniqueness of solutions is established through the application of the Krasnoselskii–Krein fixed-point framework, within which the corresponding uniqueness criteria are derived in a mathematically rigorous manner.

Before proceeding with the main analysis, we present the definitions of the types of derivatives and integrals that will be used throughout this study. The fractional derivative with exponential decay kernel [7] of the function $\kappa(\varsigma) \in H^1(0,\varsigma)$ is formulated as:

$$ {}_0^{CF}D_{\varsigma}^{\beta}\kappa(\varsigma) = \frac{1}{1-\beta}\int_0^{\varsigma}\kappa'(\zeta)\left[-\frac{\zeta}{1-\zeta}(\varsigma-\zeta)\right]\mathrm{d}\zeta, 0<\beta<1. $$

The associated integral of $\kappa(\varsigma)$ with respect to ς is given as

$$ {}^{CF}I_{\varsigma}^{\beta}\kappa(\varsigma) = (1-\beta)\kappa(\varsigma) + \beta\int_0^{\varsigma}\kappa(\zeta)\,\mathrm{d}\zeta. $$

where $\kappa(\varsigma) \in C(0,\varsigma)$. The definition of fractal derivative [8] is

$$ {}_0^{F}D_t^{\beta}\kappa(\varsigma) = \lim_{\varsigma\to\varsigma_1}\frac{\kappa(\varsigma)-\kappa(\varsigma_1)}{\varsigma^{\beta}-\varsigma_1^{\beta}}. $$

where the function $\kappa(\varsigma) \in C(0,\varsigma)$. The associated fractal integral [8] is given

by

$$ {}_0^F I_t^\beta \kappa(\varsigma) = \beta \int_0^\varsigma \zeta^{\beta-1} \kappa(\zeta)\, \mathrm{d}\zeta. $$

The definition of global derivative [2] is

$$ {}_0 D_{g(t)}^\beta \kappa(\varsigma) = \lim_{t \to t_1} \frac{\kappa(\varsigma) - \kappa(\varsigma_1)}{g(\varsigma) - g(\varsigma_1)}. $$

The associated Riemann-Stieltjes integral corresponding to global derivative [2] is given by

$$ {}_0 I_{g(t)} \kappa(\varsigma) = \int_0^\varsigma \kappa(\zeta)\, \mathrm{d}g(\zeta) $$

where the function $\kappa(\varsigma)$ is a real variable on the interval $[0, \varsigma]$. If $g(t)$ is differentiable, the definition can also be considered as follows:

$$ {}_0 I_{g(t)} \kappa(\varsigma) = \int_0^\varsigma \kappa(\zeta)\, g'(\zeta)\, \mathrm{d}\zeta. $$

2 Krasnoselskii-Krein conditions for the uniqueness of fractal differential equations

In this section, we provide a detailed discussion of the Krasnoselskii–Krein conditions [11], which are widely recognized in the literature for establishing rigorous criteria that guarantee the uniqueness of solutions to differential equations defined via fractal derivatives. These conditions offer a powerful theoretical framework for analyzing the behavior of such equations, ensuring that, under specified assumptions, the solutions are well-posed and mathematically robust. To illustrate the application of these conditions, we focus on the initial value problem formulated with a fractal derivative [8], setting the stage for both theoretical analysis and subsequent numerical investigations.

$$ {}_0^F D_t^\beta \phi(t) = f\left(t, \phi(t)\right), \quad \phi(0) = \phi_0, \tag{2.1} $$

where $0 < \beta < 1$, $f \in C(\Omega, \mathbb{R})$, $\left|f(t, \phi)\right| \leq M$ on Ω,

$$ \Omega = \left\{(t, \phi) : 0 \leq t - t_0 \leq a, |\phi - \phi_0| \leq b\right\}, $$

and $aM \leq b$. Suppose that f satisfies the following conditions on Ω:

$$ \left|f(t, \phi_1) - f(t, \phi_2)\right| \leq \frac{K\eta |\phi_1 - \phi_2|}{t^\alpha}, \quad t \neq 0, \text{ with } K\eta < \alpha, \quad K > 1; \tag{2.2} $$

$$ \left|f(t, \phi_1) - f(t, \phi_2)\right| \leq \beta |\phi_1 - \phi_2|^\rho, \quad 0 < \rho < 1, \quad K(1 - \rho) < 1 \tag{2.3} $$

where $\beta > 0$ is a constant.

By a solution of the IVP (2.1), we mean a function $\phi \in C^\alpha\left([t_0, t_0 + a], \mathbb{R}\right)$ for which the fractal derivative ${}_0^F D_t^\beta \phi(t)$ exists and satisfies (2.1). Any solution $\phi(t) = \phi(t, t_0, \phi_0)$ of (2.1) also satisfies the equivalent Volterra integral equation

$$ \phi(t) = \phi_0 + \beta \int_0^t s^{\beta-1} f\left(s, \phi(s)\right) \mathrm{d}s, \ 0 < \beta < 1 $$

on $[t_0, t_0 + a]$ and vice versa.

We shall now state our main result.

Theorem 1. *Assume that the function f in (2.1) satisfies the Krasnoselskii-Krein type conditions (2.2)) and (2.3) [11]. Then, there exists a unique solution $\phi(t) = \phi(t, t_0, \phi_0)$ of (2.1) on $[t_0, t_0 + \bar{r}]$ where $\bar{r} = \min\left\{a, \left(b/M\right)^{1/\beta}\right\}$ and the sequence of approximations $\left\{\phi_n(t)\right\}$, $\phi_n(t) \in \Omega$ for $n = 0, 1, 2, ...$, defined by*

$$\phi_{n+1}(t) = \phi_0 + \beta \int_0^t s^{\beta-1} f\left(s, \phi_n(s)\right) \mathrm{d}s, \tag{2.4}$$

converge uniformly to the unique solution $\phi(t)$ of (2.1) on $J = [t_0, t_0 + \bar{r}]$.

Proof. Choose a function $\phi_0(t), \phi_0 \in C^1\left([t_0, t_0 + a], \mathbb{R}\right)$ with $\phi_0(t_0) = \phi_0$ and $\phi_0(t) \in \Omega$. The successive approximations $\left\{\phi_n(t)\right\}$, $n = 1, 2, ...$, given by (2.4) are well defined and continuous on $[t_0, t_0+\bar{r}]$ where $\bar{r} = \min\left\{a, \left(b/M\right)^{1/\beta}\right\}$. Indeed, for $n = 1, 2, ...$, by induction, we get

$$\begin{aligned}\left|\phi_n(t) - \phi_0\right| &\le \beta \int_0^t s^{\beta-1} \left|f\left(s, \phi_{n-1}(s)\right)\right| \mathrm{d}s \\ &\le \beta \int_0^t s^{\beta-1} M \le a^\beta M \le b.\end{aligned}$$

Note that (2.4) is equivalent to

$${}_0^F D_t^\beta \phi_{n+1}(t) = f\left(t, \phi_n(t)\right), \quad \phi_n(0) = \phi_0, \tag{2.5}$$

for all $n = 1, 2, ...$ We wish to show that

$$\lim_{n\to\infty} \left|{}_0^F D_t^\beta \phi_n(t) - f\left(t, \phi_n(t)\right)\right| = 0, \text{ on } J. \tag{2.6}$$

From condition (2.3), we have $K(1-\rho) < 1$, i.e. $K < 1 + \rho \sum_{i=0}^{\infty} \rho^i$, and therefore, there exists an integer $N > 1$ such that $K < 1 + \rho \sum_{i=0}^{N-1} \rho^i$.

We have from (2.5), and the fact that $\left|f(t, \phi)\right| \le M$ on Ω,

$$\left|{}_0^F D_t^\beta \phi_1(t) - f\left(t, \phi_1(t)\right)\right| = \left|f\left(t, \phi_0(t)\right) - f\left(t, \phi_1(t)\right)\right| \le 2M \tag{2.7}$$

and for $n = 1, 2, ...$,

$$\left|{}_0^F D_t^\beta \phi_n(t) - f\left(t, \phi_n(t)\right)\right| = \left|{}_0^F D_t^\beta \phi_{n+1}(t) - {}_0^F D_t^\beta \phi_n(t)\right|.$$

In view of (2.5) and condition (2.3), we get, for $i = 1, 2, ...$,

$$\begin{aligned}&\left|{}_0^F D_t^\beta \phi_{i+1}(t) - f\left(t, \phi_{i+1}(t)\right)\right| = \left|f\left(t, \phi_i(t)\right) - f\left(t, \phi_{i+1}(t)\right)\right| \\ &\le \beta \left(\left|\phi_i(t) - \phi_{i+1}(t)\right|\right)^\rho = \beta\Big[\beta \int_0^t s^{\beta-1} \left|{}_0^F D_t^\beta \phi_i(s) - f\left(s, \phi_i(s)\right)\right| \mathrm{d}s\Big]^\rho.\end{aligned}$$

From this and (2.7), and by induction, we obtain the following estimate on J:

$$\left|{}_0^F D_t^\beta \phi_{N+1}(t) - f\left(t, \phi_{N+1}(t)\right)\right| \leq Rt^\beta \tag{2.8}$$

where $\lambda = \beta r$, $r = \rho \sum_{i=0}^{N-1} \rho^i$, $N > 1$ such that $K < 1 + r$ and

$$R = \left(\beta^{1+\rho+\rho^2+\ldots+\rho^{N-1}}\right)(2M)^{\rho^N} \tag{2.9}$$

Now, utilizing the conditions (2.2) and (2.5) we arrive at, for $j = 0, 1, 2, \ldots$ and $0 < t - t_0 \leq a$,

$$\begin{aligned}
&\left|{}_0^F D_t^\beta \phi_{N+j+1}(t) - f\left(t, \phi_{N+j+1}(t)\right)\right| \\
&\leq \frac{K\eta\beta}{t^\beta}\left|\phi_{N+j+1}(t) - \phi_{N+j}(t)\right| \\
&\leq \frac{K\eta}{t^\beta}\left[\int_0^t s^{\beta-1}\left|{}_0^F D_t^\beta \phi_{N+j}(s) - f\left(s, \phi_{N+j}(s)\right)\right| \mathrm{d}s\right]
\end{aligned}$$

and therefore, using the estimate (2.8) and the induction argument we get, for $0 < t - t_0 \leq a$ and $j = 0, 1, 2, \ldots$,

$$\left|{}_0^F D_t^\beta \phi_{N+j+1}(t) - f\left(t, \phi_{N+j+1}(t)\right)\right| \leq \left(K\eta/\beta\right)^j Rt^\beta.$$

Since $K\eta < \beta$, the claim (2.6) is proved. Thus, we have the sequence $\left\{\phi_n(t)\right\}$ with $\phi_n(t_0) = \phi_0$, $\left|\phi_n(t) - \phi_0\right| \leq b$, ${}_0^F D_t^\beta \phi_n(t)$ is continuous on $|t - t_0| \leq a$, satisfying the estimate

$$\left|{}_0^F D_t^\beta \phi_{N+j+1}(t) - f\left(t, \phi_{N+j+1}(t)\right)\right| \leq R\rho^j t^\beta \tag{2.10}$$

where $\rho = \frac{K\eta}{\beta} < 1$ and the constants R, λ and N are determined by (2.9).

We shall now show that the sequence $\left\{\phi_n(t)\right\}$ converges uniformly on $0 \leq t^\beta - t_0^\beta \leq a$. By (2.10), there exist on $|t - t_0| \leq a$ continuous functions $\rho_{N+j+1}(t)$, $j = 0, 1, 2, \ldots$, such that

$${}_0^F D_t^\beta \phi_{N+j+1}(t) = f\left(t, \phi_{N+j+1}(t)\right) + \rho_{N+j+1}(t), \tag{2.11}$$

where

$$\left|\rho_{N+j+1}(t)\right| \leq R\rho^j t^\lambda \leq R\rho^j a^\lambda \tag{2.12}$$

and

$$\phi_{N+j+1}(t) = \phi_0 + \beta \int_{t_0}^t s^{\beta-1}\left|f\left(s, \phi_{N+j}(s)\right) + \rho_{N+j+1}(s)\right| \mathrm{d}s. \tag{2.13}$$

In view of (2.5) and (2.11)–(2.13) and condition (2.3), we have

$$\Delta \leq \beta\left(\left|\phi_{N+j+1}(t) - \phi_{N+i+1}(t)\right|\right)^\rho + R\left(\rho^i + \rho^j\right)t^\beta, \tag{2.14}$$

where for convenience, we define

$$\Delta = \left|{}_0^F D_t^\beta \phi_{N+j+1}(t) - {}_0^F D_t^\beta \phi_{N+i+1}(t)\right|.$$

Since

$$\begin{aligned}\left|\phi_{N+j+1}(t) - \phi_{N+i+1}(t)\right| = \beta \int_{t_0}^{t} \Big[s^{\beta-1}\big(f\big(s, \phi_{N+j}(s)\big)\\ - f\big(s, \phi_{N+i}(s)\big)\big) + \left|\rho_{N+j+1}(s) - \rho_{N+i+1}(s)\right|\Big]\mathrm{d}s\end{aligned}$$

we get from the above, (2.14) and $\rho^i + \rho^j \leq 2$

$$\Delta \leq \beta\left(\big(2M + 2Ra^\lambda\big)/\beta\right)^\rho \left(t^\beta\right)^{\alpha\rho} + 2Rt^\beta.$$

Furthermore, since $\lambda = \alpha r$ and $\alpha\rho < \alpha r$ we obtain the estimate

$$\Delta \leq \beta\left[\left(\big(2M + 2Ra^\lambda\big)/\beta\right)^\rho + 2R\right] a^{\alpha r} \equiv R_1. \tag{2.15}$$

Again using (2.15) and proceeding as before, we have a new estimate given by

$$\Delta \leq \beta[\big(\big(R_1 + 2Ra^\lambda\big)/\beta$$

where $R_2 = \beta\left[\left((R_1 + 2Ra^\lambda)/\beta\right)^\rho + 2R\right]$.

Repeating this process $(N-1)$ times and letting R_{N-1} be an aptly chosen constant $\hat{R}$, we get for $i, j = 0, 1, 2, \ldots$ and $0 \leq t - t_0 \leq a$,

$$\Delta \leq \hat{R}t^\beta. \tag{2.16}$$

Now, condition (2.2), (2.11), (2.12) and (2.16) yield

$$\begin{aligned}\Delta &\leq \left|f\left(t, \phi_{N+j+1}(t)\right) - f\left(t, \phi_{N+i+1}(t)\right)\right| + R\left(\rho^i + \rho^j\right)t^\beta\\ &\leq \frac{K\eta}{t^\beta - t_0^\beta}\left|\phi_{N+j+1}(t) - \phi_{N+i+1}(t)\right| + R\left(\rho^i + \rho^j\right)t^\beta\end{aligned}$$

which yields to

$$\Delta \leq \left[\frac{K\eta}{\alpha}\left(\hat{R} + 2Ra^\lambda\right) + R\left(\rho^i + \rho^j\right)\right]t^\beta.$$

Identifying $\hat{R} + 2Ra^\lambda$ as R^* we can write the above in the form

$$\Delta \leq \left[\rho R^* + R\left(\rho^i + \rho^j\right)\right]t^\beta.$$

By induction we arrive at

$$\Delta \leq \left[\rho^{m-1}R^* + R\left(\rho^i + \rho^j\right)\left(\rho^{m-1} + \rho^{m-2} + \ldots + 1\right)\right]t^\beta$$

$$\leq \left[\rho^{m-1}R^* + \left(\rho^i + \rho^j\right)\frac{R}{1-\rho}\right]t^\beta.$$

This last estimate shows that $\Delta \to 0$ as $i, j, m \to \infty$ since $\rho = \frac{K\eta}{\alpha} < 1$. Hence the sequence $\left\{f\left(t, \phi_n\left(t\right)\right)\right\}$ satisfies the Cauchy criterion, the sequence $\left\{f\left(t, \phi_n\left(t\right)\right)\right\}$ is uniformly convergent on $|t - t_0| \leq a$ and, as a consequence, the sequence $\left\{\phi_n\left(t\right)\right\}$ is also uniformly convergent on $|t - t_0| \leq a$.

Let $\phi\left(t\right)$ be the limit function of $\left\{\phi_n\left(t\right)\right\}$; it is easy to see that $\phi\left(t\right)$ is the solution of (2.1). If there are two solutions $\phi\left(t\right), \psi\left(t\right)$ consider the sequence

$$\phi\left(t\right), \psi\left(t\right), \phi\left(t\right), \psi\left(t\right), ...$$

It is easy to see that this sequence is uniformly convergent and hence $\phi\left(t\right) \equiv \psi\left(t\right)$. This implies that the solution is unique. □

3 Successive midpoint formula

In this section, we present the successive midpoint method as a robust and systematic numerical technique for addressing nonlinear differential equations characterized by diverse derivative operators, including Caputo–Fabrizio, fractal, and global derivatives [5]. This method offers a unified computational framework capable of handling both local and nonlocal dynamics, thereby enabling precise approximations of complex behaviors inherent in such systems. By applying this approach, we can effectively investigate the accuracy of solutions across a wide range of derivative orders, complementing the theoretical uniqueness results established through the Krasnoselskii–Krein conditions. To achieve our aim, we start with the classical nonlinear equation

$$\begin{cases} y\prime\left(t\right) = \psi\left(t, y\left(t\right)\right) \\ y\left(0\right) = y_0 \end{cases}.$$

Applying the integral on both side yields

$$\begin{cases} y\left(t\right) = y\left(0\right) + \int_0^t \psi\left(\tau, y\left(\tau\right)\right)d\tau, \\ y\left(0\right) = y_0 \end{cases}.$$

Considering at $t = t_{n+1}$ and $t = t_n$, we have

$$y\left(t_{n+1}\right) = y\left(t_n\right) + \int_{t_n}^{t_{n+1}} \psi\left(\tau, y\left(\tau\right)\right)d\tau.$$

Note that the midpoint between t_{n+1} and t_n is $t_n + \frac{h}{2}$.Doing same procedure k times, we have the following successive midpoint formula [6]

$$y_{n+1} = y_n + \frac{h}{2^{k-1}}\sum_{j=0}^{2^{k-1}-1}\psi\left(t_n + \frac{\left(2j+1\right)h}{2^k}, y\left(t_n + \frac{\left(2j+1\right)h}{2^k}\right)\right),$$

where

$$y\left(t_n+\frac{(2j+1)\,h}{2^k}\right)=y_n+\frac{(2j+1)\,h}{2^k}\psi\left(t_n,y_n\right).$$

Note that when $k=1$, we obtain the midpoint method.

For Caputo-Fabrizio case [7], we consider a general Cauchy problem which is given by

$$\begin{cases} {}_0^{CF}D_t^{\alpha}y\left(t\right)=\psi\left(t,y\left(t\right)\right) \\ y\left(0\right)=y_0 \end{cases}.$$

Applying the integral on both side yields

$$\begin{cases} y\left(t\right)=y\left(0\right)+\left(1-\alpha\right)\psi\left(t,y\left(t\right)\right)+\alpha\int_0^t\psi\left(\tau,y\left(\tau\right)\right)d\tau, \\ y\left(0\right)=y_0 \end{cases}.$$

Considering at $t=t_{n+1}$ and $t=t_n$, we have

$$\begin{aligned} y\left(t_{n+1}\right) &= y\left(t_n\right)+\left(1-\alpha\right)\left(\psi\left(t_{n+1},y\left(t_{n+1}\right)\right)-\psi\left(t_n,y\left(t_n\right)\right)\right) \\ &\quad +\alpha\int_{t_n}^{t_{n+1}}\psi\left(\tau,y\left(\tau\right)\right)d\tau. \end{aligned}$$

By applying midpoint rule consecutively, the following numerical algorithm is obtained:

$$\begin{aligned} y_{n+1} =& y_n+\left(1-\alpha\right)\left(\psi\left(t_{n+1},\widehat{y}_{n+1}\right)-\psi\left(t_n,y_n\right)\right) \\ &+\frac{\alpha h}{2^{k-1}}\sum_{j=0}^{2^{k-1}-1}\psi\left(t_n+\frac{(2j+1)\,h}{2^k},y\left(t_n+\frac{(2j+1)\,h}{2^k}\right)\right), \end{aligned}$$

where

$$\widehat{y}_{n+1}=y_0+(1-\alpha)\psi\left(t_n,y_n\right)+\alpha h\sum_{k=0}^{n}\psi\left(t_k,y_k\right)$$

and

$$y\left(t_n+\frac{(2j+1)\,h}{2^k}\right)=y_n+\alpha\frac{(2j+1)\,h}{2^k}\psi\left(t_n,y_n\right).$$

3.1 Successive midpoint method for a general Cauchy problem with fractal derivative

In this section, we present the successive midpoint method for a general nonlinear differential equation with a fractal derivative. The mathematical equation under investigation is given as follows:

$$\begin{cases} {}_0^{F}D_t^{\beta}y\left(t\right)=\psi\left(t,y\left(t\right)\right) \\ y\left(0\right)=y_0 \end{cases}.$$

Applying the fractal integral on both sides, the above problem is converted into

$$y\left(t\right)-y\left(0\right)=\beta\int_0^t\tau^{\beta-1}\psi\left(\tau,y\left(\tau\right)\right)d\tau.$$

Taking difference of equations considered at the points $t = t_{n+1}$ and $t = t_n$,

$$y\left(t_{n+1}\right) = y\left(t_n\right) + \beta \int_{t_n}^{t_{n+1}} \tau^{\beta-1} \psi\left(\tau, y\left(\tau\right)\right) d\tau.$$

Employing the midpoint idea, we write

$$y\left(t_{n+1}\right) = y\left(t_n\right) + \beta \left[\int_{t_n}^{t_n+\frac{h}{2}} \tau^{\beta-1} \psi\left(\tau, y\left(\tau\right)\right) d\tau + \int_{t_n+\frac{h}{2}}^{t_{n+1}} \tau^{\beta-1} \psi\left(\tau, y\left(\tau\right)\right) d\tau \right].$$

Then, we calculate above as follows

$$\begin{aligned} y_{n+1} =& y_n + \beta \Big(\psi\Big(t_n + \frac{h}{4}, y\Big(t_n + \frac{h}{4}\Big)\Big) \int_{t_n}^{t_n+\frac{h}{2}} \tau^{\beta-1} d\tau \\ &+ \psi\Big(t_n + \frac{3h}{4}, y\Big(t_n + \frac{3h}{4}\Big)\Big) \int_{t_n+\frac{h}{2}}^{t_{n+1}} \tau^{\beta-1} d\tau \Big). \end{aligned}$$

Thus, we get the following numerical scheme

$$\begin{aligned} y_{n+1} \quad = \quad & y_n + \psi\left(t_n + \frac{h}{4}, y\left(t_n + \frac{h}{4}\right)\right) \left(\left(t_n + \frac{h}{2}\right)^{\beta} - t_n^{\beta} \right) \\ & + \psi\left(t_n + \frac{3h}{4}, y\left(t_n + \frac{3h}{4}\right)\right) \left(t_{n+1}^{\beta} - \left(t_n + \frac{h}{2}\right)^{\beta} \right). \end{aligned}$$

The above scheme can be arranged as follows:

$$\begin{aligned} y_{n+1} \quad = \quad & y_n + \psi\left(t_n + \frac{h}{4}, y\left(t_n + \frac{h}{4}\right)\right) h^{\beta} \left(\left(n + \frac{1}{2}\right)^{\beta} - n^{\beta} \right) \\ & + \psi\left(t_n + \frac{3h}{4}, y\left(t_n + \frac{3h}{4}\right)\right) h^{\beta} \left((n+1)^{\beta} - \left(n + \frac{1}{2}\right)^{\beta} \right). \end{aligned}$$

Applying midpoint idea again, we write

$$\begin{aligned} y\left(t_{n+1}\right) = y\left(t_n\right) + \beta \Big(& \int_{t_n}^{t_n+\frac{h}{4}} \tau^{\beta-1} \psi\left(\tau, y\left(\tau\right)\right) d\tau + \int_{t_n+\frac{h}{4}}^{t_n+\frac{h}{2}} \tau^{\beta-1} \psi\left(\tau, y\left(\tau\right)\right) d\tau \\ & + \int_{t_n+\frac{h}{2}}^{t_n+\frac{3h}{4}} \tau^{\beta-1} \psi\left(\tau, y\left(\tau\right)\right) d\tau + \int_{t_n+\frac{3h}{4}}^{t_{n+1}} \tau^{\beta-1} \psi\left(\tau, y\left(\tau\right)\right) d\tau \Big), \end{aligned}$$

and

$$\begin{aligned} y_{n+1} =& y_n + \beta\psi\Big(t_n + \frac{h}{8}, y\big(t_n + h/8\big)\Big) \int_{t_n}^{t_n+\frac{h}{4}} \tau^{\beta-1} d\tau \\ &+ \psi\Big(t_n + \frac{3h}{8}, y\big(t_n + 3h/8\big)\Big) \int_{t_n+\frac{h}{4}}^{t_n+\frac{h}{2}} \tau^{\beta-1} d\tau \end{aligned}$$

$$+\psi\Big(t_n+\frac{5h}{8},y\big(t_n+5h/8\big)\Big)\int_{t_n+\frac{h}{2}}^{t_n+\frac{3h}{4}}\tau^{\beta-1}d\tau$$
$$+\psi\Big(t_n+\frac{7h}{8},y\big(t_n+7h/8\big)\Big)\int_{t_n+\frac{3h}{4}}^{t_{n+1}}\tau^{\beta-1}d\tau.$$

Hence, we can have the following

$$\begin{aligned}y_{n+1}=&y_n+\psi\Big(t_n+\frac{h}{8},y\big(t_n+h/8\big)\Big)h^\beta\left(\big(n+1/4\big)^\beta-n^\beta\right)\\&+\psi\Big(t_n+\frac{3h}{8},y\big(t_n+3h/8\big)\Big)h^\beta\left(\big(n+1/2\big)^\beta-\big(n+1/4\big)^\beta\right)\\&+\psi\Big(t_n+\frac{5h}{8},y\big(t_n+5h/8\big)\Big)h^\beta\left(\big(n+3/4\big)^\beta-\big(n+1/2\big)^\beta\right)\\&+\psi\Big(t_n+\frac{7h}{8},y\big(t_n+7h/8\big)\Big)h^\beta\left(\big(n+1\big)^\beta-\big(n+3/4\big)^\beta\right).\end{aligned}$$

Using the idea k times, we get the successive midpoint idea [4,5]

$$\begin{aligned}y_{n+1}&=y_n+\sum_{j=0}^{2^{k-1}-1}\psi\left(t_n+\frac{(2j+1)\,h}{2^k},y\left(t_n+\frac{(2j+1)\,h}{2^k}\right)\right)\\&\quad\times\left(\left(t_n+\frac{(j+1)\,h}{2^{k-1}}\right)^\beta-\left(t_n+\frac{jh}{2^{k-1}}\right)^\beta\right).\end{aligned}$$

The above is rewritten as follows:

$$\begin{aligned}y_{n+1}&=y_n+\sum_{j=0}^{2^{k-1}-1}\psi\left(t_n+\frac{(2j+1)\,h}{2^k},y\left(t_n+\frac{(2j+1)\,h}{2^k}\right)\right)\\&\quad\times h^\beta\left(\left(n+\frac{j+1}{2^{k-1}}\right)^\beta-\left(n+\frac{j}{2^{k-1}}\right)^\beta\right).\end{aligned}$$

3.2 Successive midpoint method for a general Cauchy problem with global derivative

To adapt the suggested scheme for global case, we consider a general Cauchy problem which is given by

$$\begin{cases}{}_0D_g y\,(t)=\psi\left(t,y\,(t)\right)\\ y\,(0)=y_0\end{cases}.$$

Applying the integral on both side yields

$$y\,(t)=y\,(0)+\int_0^t\psi\left(\tau,y\,(\tau)\right)g'\,(\tau)\,d\tau,\quad y\,(0)=y_0.$$

Considering at $t=t_{n+1}$ and $t=t_n$, we have

$$y\,(t_{n+1})=y\,(t_n)+\int_{t_n}^{t_{n+1}}\psi\left(\tau,y\,(\tau)\right)g'\,(\tau)\,d\tau.$$

Employing the midpoint idea, we write

$$y(t_{n+1}) = y(t_n) + \int_{t_n}^{t_n+\frac{h}{2}} \psi\left(\tau, y(\tau)\right) g'(\tau)\, d\tau + \int_{t_n+\frac{h}{2}}^{t_{n+1}} \psi\left(\tau, y(\tau)\right) g'(\tau)\, d\tau.$$

Then, we calculate above as follows

$$\begin{aligned} y_{n+1} &= y_n + \psi\left(t_n + \frac{h}{4}, y\left(t_n + \frac{h}{4}\right)\right) \int_{t_n}^{t_n+\frac{h}{2}} g'(\tau)\, d\tau \\ &\quad + \psi\left(t_n + \frac{3h}{4}, y\left(t_n + \frac{3h}{4}\right)\right) \int_{t_n+\frac{h}{2}}^{t_{n+1}} g'(\tau)\, d\tau. \end{aligned}$$

Thus, we get the following numerical scheme

$$\begin{aligned} y_{n+1} &= y_n + \psi\left(t_n + \frac{h}{4}, y\left(t_n + \frac{h}{4}\right)\right)\left(g\left(t_n + \frac{h}{2}\right) - g(t_n)\right) \\ &\quad + \psi\left(t_n + \frac{3h}{4}, y\left(t_n + \frac{3h}{4}\right)\right)\left(g(t_{n+1}) - g\left(t_n + \frac{h}{2}\right)\right). \end{aligned}$$

Applying the associated idea again, we have the following

$$\begin{aligned} y(t_{n+1}) =& y(t_n) + \int_{t_n}^{t_n+\frac{h}{4}} \psi\left(\tau, y(\tau)\right) g'(\tau)\, d\tau + \int_{t_n+\frac{h}{4}}^{t_n+\frac{h}{2}} \psi\left(\tau, y(\tau)\right) g'(\tau)\, d\tau \\ &+ \int_{t_n+\frac{h}{2}}^{t_n+\frac{3h}{4}} \psi\left(\tau, y(\tau)\right) g'(\tau)\, d\tau + \int_{t_n+\frac{3h}{4}}^{t_{n+1}} \psi\left(\tau, y(\tau)\right) g'(\tau)\, d\tau, \\ y_{n+1} =& y_n + \psi\Big(t_n + \frac{h}{8}, y\left(t_n + h/8\right)\Big) \int_{t_n}^{t_n+\frac{h}{4}} g'(\tau)\, d\tau \\ &+ \psi\Big(t_n + \frac{3h}{8}, y\left(t_n + 3h/8\right)\Big) \int_{t_n+\frac{h}{4}}^{t_n+\frac{h}{2}} g'(\tau)\, d\tau \\ &+ \psi\Big(t_n + \frac{5h}{8}, y\left(t_n + 5h/8\right)\Big) \int_{t_n+\frac{h}{2}}^{t_n+\frac{3h}{4}} g'(\tau)\, d\tau \\ &+ \psi\Big(t_n + \frac{7h}{8}, y\left(t_n + 7h/8\right)\Big) \int_{t_n+\frac{3h}{4}}^{t_{n+1}} g'(\tau)\, d\tau. \end{aligned}$$

Then, we have the following numerical scheme

$$\begin{aligned} y_{n+1} &= y_n + \psi\left(t_n + \frac{h}{8}, y\left(t_n + \frac{h}{8}\right)\right)\left(g\left(t_n + \frac{h}{4}\right) - g(t_n)\right) \\ &\quad + \psi\left(t_n + \frac{3h}{8}, y\left(t_n + \frac{3h}{8}\right)\right)\left(g\left(t_n + \frac{h}{2}\right) - g\left(t_n + \frac{h}{4}\right)\right) \\ &\quad + \psi\left(t_n + \frac{5h}{8}, y\left(t_n + \frac{5h}{8}\right)\right)\left(g\left(t_n + \frac{3h}{4}\right) - g\left(t_n + \frac{h}{2}\right)\right) \end{aligned}$$

$$+\psi\left(t_n+\frac{7h}{8},y\left(t_n+\frac{7h}{8}\right)\right)\left(g\left(t_{n+1}\right)-g\left(t_n+\frac{3h}{4}\right)\right).$$

By applying midpoint rule consecutively, the following numerical algorithm is obtained:

$$\begin{aligned}y_{n+1}=&y_n+\sum_{j=0}^{2^{k-1}-1}\psi\left(t_n+\frac{(2j+1)\,h}{2^k},y\left(t_n+\frac{(2j+1)\,h}{2^k}\right)\right)\\&\times\left[g\left(t_n+\frac{(j+1)\,h}{2^k}\right)-g\left(t_n+\frac{jh}{2^k}\right)\right],\end{aligned}$$

where

$$y\left(t_n+\frac{(2j+1)\,h}{2^k}\right)=y_n+\psi(t_n,y_n)\left(g\left(t_n+\frac{(2j+1)\,h}{2^k}\right)-g\left(t_n+\frac{jh}{2^k}\right)\right).$$

4 Application to chaos

In this section, we adapt the proposed method for the solution of chaotic systems with classical and Caputo-Fabrizio derivatives.

Example 1. We first consider a chaotic system introduced by Lai et.al [12]

$$\begin{cases}x'(t)=ax-2yz\\y'(t)=-by+2xz\\z'(t)=-cz+xyz+d/2\\x(0)=x_0,y(0)=y_0,z(0)=z_0\end{cases}.$$

For simplification, we write

$$\begin{cases}x'(t)=f_1(x,y,z,t)\\y'(t)=f_2(x,y,z,t)\\z'(t)=f_3(x,y,z,t)\end{cases}.$$

The numerical solution of the considered chaotic model is presented as [4]:

$$x_{n+1}=x_n+\frac{h}{2^{k-1}}\sum_{j=0}^{2^{k-1}-1}f_1\left(\begin{array}{c}t_n+\frac{(2j+1)h}{2^k},x\left(t_n+\frac{(2j+1)h}{2^k}\right),\\y\left(t_n+\frac{(2j+1)h}{2^k}\right),z\left(t_n+\frac{(2j+1)h}{2^k}\right)\end{array}\right),$$

$$y_{n+1}=y_n+\frac{h}{2^{k-1}}\sum_{j=0}^{2^{k-1}-1}f_2\left(\begin{array}{c}t_n+\frac{(2j+1)h}{2^k},x\left(t_n+\frac{(2j+1)h}{2^k}\right),\\y\left(t_n+\frac{(2j+1)h}{2^k}\right),z\left(t_n+\frac{(2j+1)h}{2^k}\right)\end{array}\right),$$

$$z_{n+1}=z_n+\frac{h}{2^{k-1}}\sum_{j=0}^{2^{k-1}-1}f_3\left(\begin{array}{c}t_n+\frac{(2j+1)h}{2^k},x\left(t_n+\frac{(2j+1)h}{2^k}\right),\\y\left(t_n+\frac{(2j+1)h}{2^k}\right),z\left(t_n+\frac{(2j+1)h}{2^k}\right)\end{array}\right),$$

where

$$\begin{cases} x\left(t_n+\frac{(2j+1)h}{2^k}\right)=x_n+\frac{(2j+1)h}{2^k}f_1\left(t_n,x_n,y_n,z_n\right) \\ y\left(t_n+\frac{(2j+1)h}{2^k}\right)=y_n+\frac{(2j+1)h}{2^k}f_2\left(t_n,x_n,y_n,z_n\right) \\ z\left(t_n+\frac{(2j+1)h}{2^k}\right)=z_n+\frac{(2j+1)h}{2^k}f_3\left(t_n,x_n,y_n,z_n\right) \end{cases}.$$

The presented chaotic system has chaotic properties with the following parameters and initial conditions:

$$a=2,\ \ b=8,\ \ c=2.9,\ \ d=4,$$
$$x\left(0\right)=\pm1,\ \ y\left(0\right)=\pm1,\ \ z\left(0\right)=1.$$

The numerical simulations for the considered chaotic model with classical derivative are presented in Figure 1.

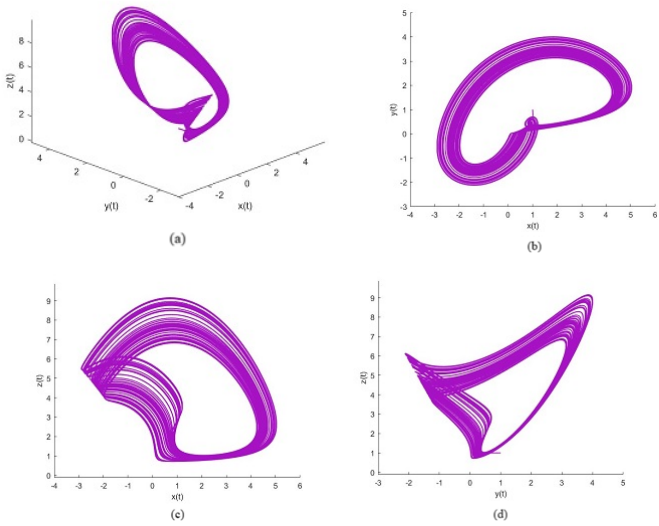

Figure 1. Numerical solution of the considered chaotic system using the considered method with classical derivative.

Figure 1 depicts the numerical solution of the investigated chaotic system obtained under the classical derivative. The three-dimensional trajectory and its two-dimensional projections reveal a well-defined chaotic attractor characterized by bounded yet highly irregular oscillations. The orbits exhibit continuous stretching and folding, reflecting the system's strong sensitivity to initial conditions. The smoothness and coherence of the attractor structure confirm that the proposed numerical scheme accurately reproduces the intrinsic chaotic dynamics of the system in the classical (integer-order) framework.

Example 2. For Caputo-Fabrizio case, we consider Thomas attractor [9] which is given by

$$\begin{cases} {}_0^{CF}D_t^{\alpha} x(t) = \sin\left(\exp(y)\right) - 0.2x \\ {}_0^{CF}D_t^{\alpha} y(t) = \cos\left(\sin(z)\right) - 0.2y \\ {}_0^{CF}D_t^{\alpha} z(t) = \exp\left(\cos(x)\right) - 0.2z \end{cases},$$

where initial conditions are taken as:

$$x(0) = 0, \quad y(0) = 3, \quad z(0) = 11.$$

By using the suggested method, the above system is solved numerically as follows

$$\begin{aligned} x_{n+1} &= x_n + (1-\alpha)\left(f_1(t_{n+1}, \widehat{x}_{n+1}, \widehat{y}_{n+1}, \widehat{z}_{n+1}) - f_1(t_n, x_n, y_n, z_n)\right) \\ &\quad + \tfrac{\alpha h}{2^{k-1}} \sum_{j=0}^{2^{k-1}-1} f_1 \begin{pmatrix} t_n + \frac{(2j+1)h}{2^k}, x\left(t_n + \frac{(2j+1)h}{2^k}\right), \\ y\left(t_n + \frac{(2j+1)h}{2^k}\right), z\left(t_n + \frac{(2j+1)h}{2^k}\right) \end{pmatrix}, \\ y_{n+1} &= y_n + (1-\alpha)\left(f_2(t_{n+1}, \widehat{x}_{n+1}, \widehat{y}_{n+1}, \widehat{z}_{n+1}) - f_2(t_n, x_n, y_n, z_n)\right) \\ &\quad + \tfrac{\alpha h}{2^{k-1}} \sum_{j=0}^{2^{k-1}-1} f_2 \begin{pmatrix} t_n + \frac{(2j+1)h}{2^k}, x\left(t_n + \frac{(2j+1)h}{2^k}\right), \\ y\left(t_n + \frac{(2j+1)h}{2^k}\right), z\left(t_n + \frac{(2j+1)h}{2^k}\right) \end{pmatrix}, \\ z_{n+1} &= z_n + (1-\alpha)\left(f_3(t_{n+1}, \widehat{x}_{n+1}, \widehat{y}_{n+1}, \widehat{z}_{n+1}) - f_3(t_n, x_n, y_n, z_n)\right) \\ &\quad + \tfrac{\alpha h}{2^{k-1}} \sum_{j=0}^{2^{k-1}-1} f_3 \begin{pmatrix} t_n + \frac{(2j+1)h}{2^k}, x\left(t_n + \frac{(2j+1)h}{2^k}\right), \\ y\left(t_n + \frac{(2j+1)h}{2^k}\right), z\left(t_n + \frac{(2j+1)h}{2^k}\right) \end{pmatrix}, \end{aligned}$$

where

$$\begin{aligned} \widehat{x}_{n+1} &= x_0 + (1-\alpha) f_1(t_n, x_n, y_n, z_n) + \alpha h \sum_{k=0}^{n} f_1(t_k, x_k, y_k, z_k), \\ \widehat{y}_{n+1} &= y_0 + (1-\alpha) f_2(t_n, x_n, y_n, z_n) + \alpha h \sum_{k=0}^{n} f_2(t_k, x_k, y_k, z_k), \\ \widehat{z}_{n+1} &= z_0 + (1-\alpha) f_3(t_n, x_n, y_n, z_n) + \alpha h \sum_{k=0}^{n} f_3(t_k, x_k, y_k, z_k), \end{aligned}$$

and

$$\begin{aligned} x\left(t_n + \frac{(2j+1)h}{2^k}\right) &= x_n + \frac{\alpha(2j+1)h}{2^k} f_1(t_n, x_n, y_n, z_n), \\ y\left(t_n + \frac{(2j+1)h}{2^k}\right) &= y_n + \frac{\alpha(2j+1)h}{2^k} f_2(t_n, x_n, y_n, z_n), \\ z\left(t_n + \frac{(2j+1)h}{2^k}\right) &= z_n + \frac{\alpha(2j+1)h}{2^k} f_3(t_n, x_n, y_n, z_n). \end{aligned}$$

The numerical simulations for the considered chaotic model with Caputo-Fabrizio derivative are presented in Figure 2.

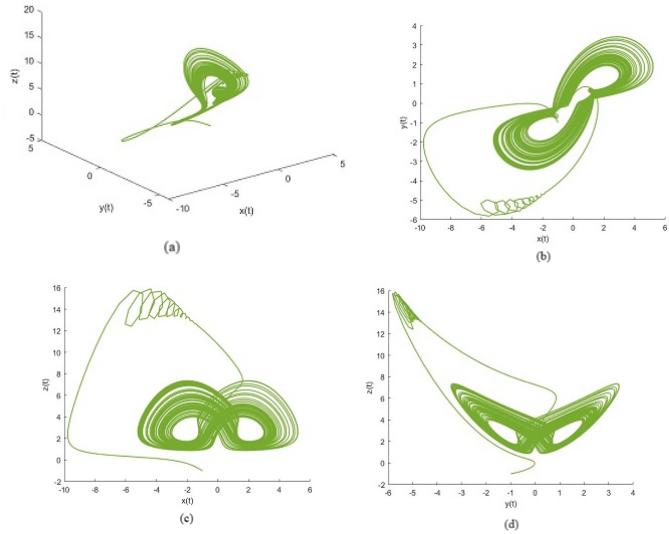

Figure 2. Graphical representation of Thomas' attractor using the considered method with the Caputo-Fabrizio derivative for $\alpha = 0.95$.

Figure 2 presents the graphical representation of Thomas' attractor computed using the Caputo–Fabrizio fractional derivative. Owing to the exponential kernel of the CF operator, the resulting trajectories demonstrate more regular, attenuated oscillations compared to the classical case. The three-dimensional plots indicate that the orbits cluster more tightly around the core of the attractor, while the two-dimensional projections display reduced amplitude variations. These features illustrate the damping effect introduced by the CF derivative, whereby the incorporated memory smooths the system's evolution and moderates its chaotic fluctuations.

Example 3. We next consider a chaotic system which incorporates a memristor with cubic monotonic nonlinearity and negative feedback control. The chaotic model presented by M.A Qureshi [13] is given by

$$\begin{aligned}
{}_0^F D_t^{\beta} \eta_1(t) &= -a\eta_1 + a\eta_2 + b\big(a_1 + b_1\eta_2^2\big)\eta_2 + c\sin(t), \\
{}_0^F D_t^{\beta} \eta_2(t) &= d_1\eta_1 - \eta_1\eta_3 - d_2\eta_2, \\
{}_0^F D_t^{\beta} \eta_3(t) &= \eta_1\eta_2 - e\eta_3.
\end{aligned}$$

The chaotic equation includes a sinusoidal function with amplitude parameters a and c. For simplicity, we write the above system as follows:

$$\begin{aligned}
{}_0^F D_t^{\beta} \eta_1(t) &= \psi_1(t;\eta_1,\eta_2,\eta_3), \\
{}_0^F D_t^{\beta} \eta_2(t) &= \psi_2(t;\eta_1,\eta_2,\eta_3), \\
{}_0^F D_t^{\beta} \eta_3(t) &= \psi_3(t;\eta_1,\eta_2,\eta_3),
\end{aligned}$$

where

$$\begin{aligned}
\psi_1(t;\eta_1,\eta_2,\eta_3) &= -a\eta_1 + a\eta_2 + b\left(a_1 + b_1\eta_2^2\right)\eta_2 + c\sin(t),\\
\psi_2(t;\eta_1,\eta_2,\eta_3) &= d_1\eta_1 - \eta_1\eta_3 - d_2\eta_2,\\
\psi_3(t;\eta_1,\eta_2,\eta_3) &= \eta_1\eta_2 - e\eta_3.
\end{aligned}$$

The numerical scheme based on successive midpoint method is achieved for the above system as follows:

$$\begin{aligned}
\eta_1^{n+1} =& \eta_1^n + \sum_{j=0}^{2^{k-1}-1} \psi_1 \begin{pmatrix} t_n + \frac{(2j+1)h}{2^k}, \eta_1\left(t_n + \frac{(2j+1)h}{2^k}\right), \\ \eta_2\left(t_n + \frac{(2j+1)h}{2^k}\right), \eta_3\left(t_n + \frac{(2j+1)h}{2^k}\right) \end{pmatrix} \\
&\times h^\beta \left(\left(n + (j+1)/2^{k-1}\right)^\beta - \left(n + j/2^{k-1}\right)^\beta\right),\\
\eta_2^{n+1} =& \eta_2^n + \sum_{j=0}^{2^{k-1}-1} \psi_2 \begin{pmatrix} t_n + \frac{(2j+1)h}{2^k}, \eta_1\left(t_n + \frac{(2j+1)h}{2^k}\right), \\ \eta_2\left(t_n + \frac{(2j+1)h}{2^k}\right), \eta_3\left(t_n + \frac{(2j+1)h}{2^k}\right) \end{pmatrix} \\
&\times h^\beta \left(\left(n + \frac{j+1}{2^{k-1}}\right)^\beta - \left(n + \frac{j}{2^{k-1}}\right)^\beta\right),\\
\eta_3^{n+1} =& \eta_3^n + \sum_{j=0}^{2^{k-1}-1} \psi_3 \begin{pmatrix} t_n + \frac{(2j+1)h}{2^k}, \eta_1\left(t_n + \frac{(2j+1)h}{2^k}\right), \\ \eta_2\left(t_n + \frac{(2j+1)h}{2^k}\right), \eta_3\left(t_n + \frac{(2j+1)h}{2^k}\right) \end{pmatrix} \\
&\times h^\beta \left(\left(n + \frac{j+1}{2^{k-1}}\right)^\beta - \left(n + \frac{j}{2^{k-1}}\right)^\beta\right).
\end{aligned}$$

The numerical simulations for the considered chaotic model with fractal derivative are presented in Figure 3.

Figure 3 illustrates the numerical visualization of the memristor-based chaotic system governed by the fractal derivative. The introduction of fractal calculus leads to a trajectory with markedly more intricate and densely layered structures. The projections reveal pronounced oscillatory behavior and spiral formations that collectively suggest a multi-scale chaotic response. The increased complexity and irregularity of the phase-space patterns highlight the significant role of the fractal derivative in enhancing the system's sensitivity and generating a fractal-like attractor.

Example 4. For global case, we reconsider the following system in Example 3

$$\begin{aligned}
{}_0D_g\eta_1(t) &= \psi_1(t;\eta_1,\eta_2,\eta_3),\\
{}_0D_g\eta_2(t) &= \psi_2(t;\eta_1,\eta_2,\eta_3),\\
{}_0D_g\eta_3(t) &= \psi_3(t;\eta_1,\eta_2,\eta_3),
\end{aligned}$$

where the function $g(t)$ is chosen as $0.92t$. Such system can be solved by the

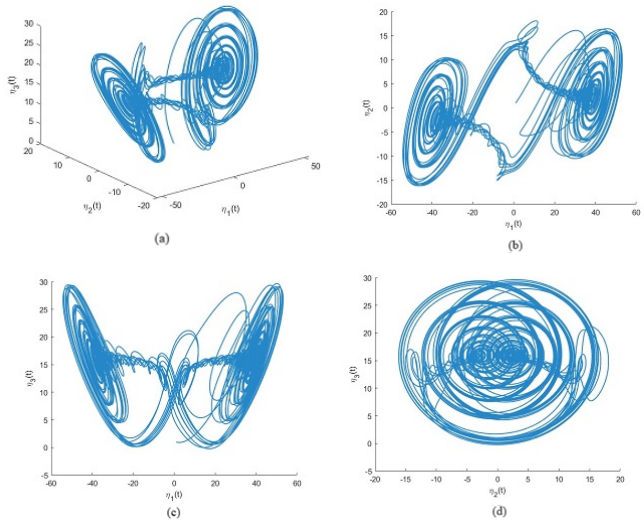

Figure 3. Numerical visualization of memristor system with fractal derivative for $\beta = 0.9$.

following scheme:

$$\eta_1^{n+1} = \eta_1^n + \sum_{j=0}^{2^{k-1}-1} \psi_1 \begin{pmatrix} t_n + \frac{(2j+1)h}{2^k}, \eta_1\left(t_n + \frac{(2j+1)h}{2^k}\right), \\ \eta_2\left(t_n + \frac{(2j+1)h}{2^k}\right), \eta_3\left(t_n + \frac{(2j+1)h}{2^k}\right) \end{pmatrix} \times \left[g\left(t_n + \frac{(j+1)h}{2^k}\right) - g\left(t_n + \frac{jh}{2^k}\right) \right],$$

$$\eta_2^{n+1} = \eta_2^n + \sum_{j=0}^{2^{k-1}-1} \psi_2 \begin{pmatrix} t_n + \frac{(2j+1)h}{2^k}, \eta_1\left(t_n + \frac{(2j+1)h}{2^k}\right), \\ \eta_2\left(t_n + \frac{(2j+1)h}{2^k}\right), \eta_3\left(t_n + \frac{(2j+1)h}{2^k}\right) \end{pmatrix} \times \left[g\left(t_n + \frac{(j+1)h}{2^k}\right) - g\left(t_n + \frac{jh}{2^k}\right) \right],$$

$$\eta_3^{n+1} = \eta_3^n + \sum_{j=0}^{2^{k-1}-1} \psi_3 \begin{pmatrix} t_n + \frac{(2j+1)h}{2^k}, \eta_1\left(t_n + \frac{(2j+1)h}{2^k}\right), \\ \eta_2\left(t_n + \frac{(2j+1)h}{2^k}\right), \eta_3\left(t_n + \frac{(2j+1)h}{2^k}\right) \end{pmatrix} \times \left[g\left(t_n + \frac{(j+1)h}{2^k}\right) - g\left(t_n + \frac{jh}{2^k}\right) \right].$$

The numerical simulations for the considered chaotic model with global derivative are presented in Figure 4. Figure 4 illustrates the numerical phase-space representation of the memristor-based chaotic system under the assumption of a global derivative operator. The three-dimensional phase portrait along with its two-dimensional projections reveals trajectories that remain confined within a bounded region of the phase space, while exhibiting complex, interlaced oscillations and intricate looping — behavior characteristic of a strange attractor.

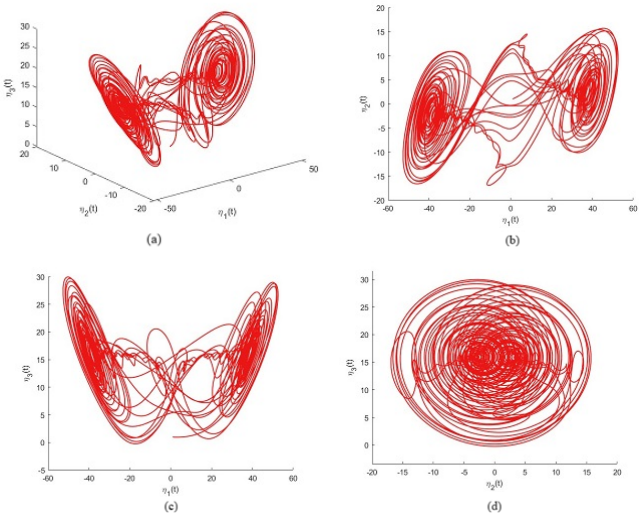

Figure 4. Numerical visualization of memristor system with global derivative for $g(t) = 0.92t$.

Such bounded yet highly irregular dynamics strongly suggest that the system retains its chaotic nature even when the classical derivative is replaced by a global derivative.

5 Conclusions

This study provides an extensive theoretical and numerical investigation of differential equations involving classical, fractal, global, and Caputo–Fabrizio derivative operators, thereby contributing to the ongoing development of generalized calculus frameworks. On the theoretical side, particular emphasis is placed on the analysis of fractal differential equations. By employing the Krasnoselskii–Krein fixed-point framework, uniqueness conditions for their solutions are established, offering a mathematically robust foundation for the well-posedness of fractal dynamical models. This theoretical advancement clarifies the structural behavior induced by fractal operators and provides essential criteria for ensuring the reliability of subsequent numerical computations.

From the numerical viewpoint, the successive midpoint method—initially formulated for classical and Caputo–Fabrizio derivatives—is systematically extended to encompass fractal and global derivatives. This generalization broadens the applicability of the method to nonlocal and memory-dependent operators capable of describing significantly more intricate system dynamics. A detailed description of the implementation is provided, including the discretization strategy, subdivision of computational intervals, and the midpoint-based iterative construction of approximate solutions, thus establishing a coherent computational framework suitable for a wide class of differential models.

The numerical performance of the extended method is rigorously assessed through a series of simulations conducted on representative chaotic systems equipped with different types of derivative operators. The classical derivative case yields a well-structured chaotic attractor with smooth, intertwined trajectories, demonstrating that the method faithfully reproduces the intrinsic chaotic nature of the underlying system. In contrast, simulations performed with the Caputo–Fabrizio derivative exhibit smoother transitions and more tightly clustered trajectories, reflecting the damping and memory effects imparted by its exponential kernel. Meanwhile, the memristor system governed by the fractal derivative generates significantly more intricate and densely layered structures, illustrating the rich multi-scale behavior induced by fractal calculus. These distinct graphical patterns across Figures 1–4 collectively confirm that the successive midpoint method is sufficiently flexible to capture both classical chaotic oscillations and the modified dynamical regimes arising from generalized derivatives. Comparative analyses further demonstrate the method's stability, reliability, and accuracy across a wide range of operator types and derivative orders.

Overall, the findings demonstrate that the successive midpoint method constitutes a robust, adaptable, and computationally efficient approach for solving differential equations involving both classical and generalized derivative operators. By integrating rigorous theoretical guarantees of uniqueness with a versatile numerical scheme, this study helps bridge the gap between the mathematical foundations of generalized differentiation and their practical utility in modeling complex dynamical phenomena. The results also point toward several promising directions for future research, including the extension of the method to stochastic generalized-operator systems, the construction of higher-order midpoint-based schemes, and the application of the framework to multi-scale or high-dimensional chaotic models.

Acknowledgements

The authors are very grateful to anonymous reviewer for carefully reading the paper and for very useful discussions and suggestions which have improved the paper.

References

[1] H.F. Ahmed. Fractional Euler method: An effective tool for solving fractional differential equations. *Journal of the Egyptian Mathematical Society*, **26**(1):38–43, 2018. https://doi.org/10.21608/JOEMS.2018.9460.

[2] A. Atangana. Extension of rate of change concept: From local to non-local operators with applications. *Results in Physics*, **19**:103515, 2020. https://doi.org/10.1016/j.rinp.2020.103515.

[3] A. Atangana and S.I. Araz. Nonlinear equations with global differential and integral operators: Existence, uniqueness with application to epidemiology. *Results in Physics*, **20**:103593, 2021. https://doi.org/10.1016/j.rinp.2020.103593.

[4] A. Atangana and S.I. Araz. A successive midpoint method for nonlinear differential equations with classical and Caputo–Fabrizio derivatives. *AIMS Mathematics*, **8**(11):27309–27327, 2023. https://doi.org/10.3934/math.20231397.

[5] A. Atangana and S.I. Araz. Extension of successive midpoint scheme for nonlinear differential equations with global nonlocal operators. *Alexandria Engineering Journal*, **111**:374–384, 2025. https://doi.org/10.1016/j.aej.2024.10.013.

[6] A. Atangana and S. İğret Araz. A successive midpoint method for nonlinear differential equations with classical and Caputo–Fabrizio derivatives. *AIMS Mathematics*, **8**(11):27309–27327, 2023. https://doi.org/10.3934/math.20231397.

[7] M. Caputo and M. Fabrizio. A new definition of fractional derivative without singular kernel. *Progress in Fractional Differentiation and Applications*, **1**(2):73–85, 2015. https://doi.org/10.12785/pfda/010201.

[8] W. Chen. Time–space fabric underlying anomalous diffusion. *Chaos, Solitons & Fractals*, **28**(4):923–929, 2006. https://doi.org/10.1016/j.chaos.2005.08.199.

[9] B. Ghanbari and K.S. Nisar. Some effective numerical techniques for chaotic systems involving fractal–fractional derivatives with different laws. *Frontiers in Physics*, **8**:192, 2020. https://doi.org/10.3389/fphy.2020.00192.

[10] J.F. Gómez-Aguilar, M.K. Naik, R. George, C. Baishya, İ. Avcı and E. Pérez-Careta. Chaos and stability of a fractional model of the cyber ecosystem. *AIMS Mathematics*, **9**(8):22146–22173, 2024. https://doi.org/10.3934/math.20241077.

[11] M.A. Krasnoselskii and S.G. Krein. On a class of uniqueness theorems for the equation y' = f(x,y). *Uspekhi Matematicheskikh Nauk*, **11**(1):209–213, 1956.

[12] Q. Lai, A. Akgul, C. Li, G. Xu and Ü. Çavuşoğlu. A new chaotic system with multiple attractors: Dynamic analysis, circuit realization and s-box design. *Entropy*, **20**(1):12, 2018. https://doi.org/10.3390/e20010012.

[13] M.A. Qureshi and N.A. Khan. Clown face in 3D chaotic system integrated with memristor electronics, DNA encryption and fractional calculus. *European Physical Journal B*, **97**:63, 2024. https://doi.org/10.1140/epjb/s10051-024-00694-4.